ChemComm

COMMUNICATION

View Article Online
View Journal | View Issue

Cite this: *Chem. Commun.*, 2018, **54**, 156

Received 27th August 2017,
Accepted 21st September 2017

DOI: 10.1039/c7cc06714c

rsc.li/chemcomm

Trigonal columnar self-assembly of bent phasmid mesogens†

Huifang Cheng,‡[a] Ya-xin Li,‡[b] Xiang-bing Zeng,[b] Hongfei Gao,[a] Xiaohong Cheng *[a] and Goran Ungar *[bc]

Three compounds with a bent rod-like aromatic core and with three alkoxy chains at each end were synthesised by click reaction. The compounds form a columnar liquid crystal phase with non-centrosymmetric trigonal *p*31*m* symmetry, the columns having a 3-arm star-like cross-section.

The term "phasmid" mesogen is used to describe rod-like molecules with three flexible chains, usually alkyl, at each end, and the name refers to the similarity with the six-legged insects known by the same name.[1] Usually such mesogens form the hexagonal columnar (Col_{hex}) liquid crystal (LC) phase, where typically three aromatic rods lie parallel to each other and perpendicular to the column axis, forming a stratum of the column; the alkyls fill the space between the columns.[2] Phasmids are a subclass of a wider class of rod-like molecules with more than one chain at each end, known as polycatenar mesogens. Columnar phases, particularly the most commonly observed hexagonal phase, are normally assembled from disk-like or fan-shaped molecules.[3–7] Alternatively a variety of "honeycomb" columnar phases are seen in rod-like amphiphiles with flexible side-chains.[8,9] One may ask why phasmidic columns, with elongated rods lying normal to the column axis, pack on a lattice with hexagonal symmetry, when such packing is normally reserved for round cylinders or hexagonal prisms. The answer may be in that the successive strata in a column are rotated, forming a helix, making the averaged cross-section circular. Such helical twist of polycatenar strata has recently been suggested by the observation of chirality in non-chiral polycatenar compounds in the triple-network cubic phase, where the networks are also made up of short column segments.[10] Columns made up of more circular strata, containing discotic or fan-shaped mesogens, are also understood to feature helical twist.[11–14]

The question we address here is whether a trigonal columnar LC phase can be formed, with three-fold rather than six-fold symmetry and with non-cylindrical columns. In honeycomb-like inverted columnar phases of side-chain-containing rod-like amphiphiles, in some cases the cross-section of the prismatic channels with aromatic walls is hexagonal; thus although the columns are not circular, naturally the symmetry is still hexagonal, plane group *p*6*mm*.[8,9] However, in two cases amphiphiles of that kind were reported to form honeycombs with only three-fold symmetry (see below).[15,16] Such non-centrosymmetric structures are rare in liquid crystals but are of interest for their potential ferroelectric, pyroelectric or non-linear optical properties. The question remains whether such three-fold symmetry is possible in the more conventional columnar phases where the hard aromatic moieties occupy the centre, rather than the periphery of the column. Here we show that columns with a three-arm star cross-section and trigonal symmetry can form from bent-core, or banana-shaped phasmids. While the crystallographic plane group belongs to the hexagonal system, the phase symmetry is actually trigonal.

The aromatic rod-like core in the compounds described here have a bend of 109° in the centre due to the sp^3-hybridized methylene group – see Scheme 1. The compounds are labelled **IC^3/*n***, with n = 10, 12, 14 the number of carbon atoms in each of the six terminal alkyl chains. They were synthesized by a Cu(I)-catalyzed click reaction.[17] All three compounds display a liquid crystal phase, with the texture recorded by polarized optical microscopy (POM) featuring clear developable domains ("spherulites"),[18] typical of a columnar LC phase – see Fig. 1. The transition temperatures and heats of transition on 1st heating, cooling and 2nd heating, determined by DSC in combination with X-ray diffraction and nonlinear optical

[a] *Key Laboratory of Medicinal Chemistry for Natural Resources, Chemistry Department, Yunnan University, Yunnan, 650091, P. R. China. E-mail: xhcheng@ynu.edu.cn*
[b] *Department of Materials Science and Engineering, University of Sheffield, Sheffield, S1 3JD, UK. E-mail: g.ungar@sheffield.ac.uk*
[c] *Department of Physics, Zhejiang Sci-Tech University, Xiasha College Park, Zhejiang, 310018, China*

† Electronic supplementary information (ESI) available: Synthesis, analytical data, molecular simulation video. See DOI: 10.1039/c7cc06714c

‡ Both authors contributed equally to this work.

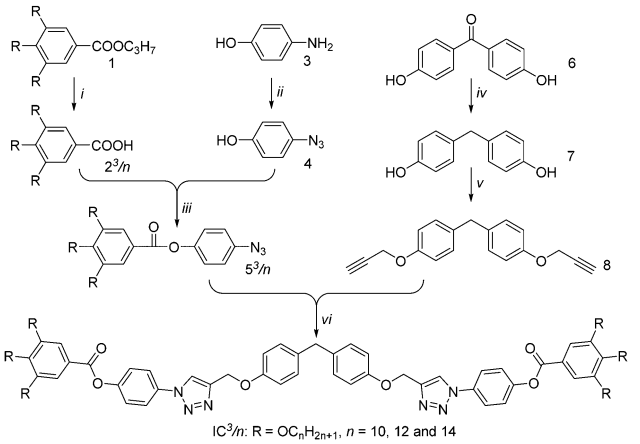

Scheme 1 Synthesis of compounds **IC^3/*n***. *Reagents and conditions*: (i) KOH, CH_3CH_2OH, reflux, overnight; (ii) (a) $NaNO_2$/HCl, 0 °C, 1 h; (b) NaN_3, 0–5 °C, 5 h; (iii) dicyclohexylcarbodiimide, 4-dimethylaminopyridine, CH_2Cl_2, 0–5 °C, 18 h; (iv) $LiAlH_4$, $AlCl_3$, THF, 65 °C, 48 h; (v) KOH, propargyl bromide, acetone, reflux; (vi) *tert*-butanol, THF, H_2O, sodium ascorbate, $CuSO_4{\cdot}5H_2O$, 25 °C, 20 h.

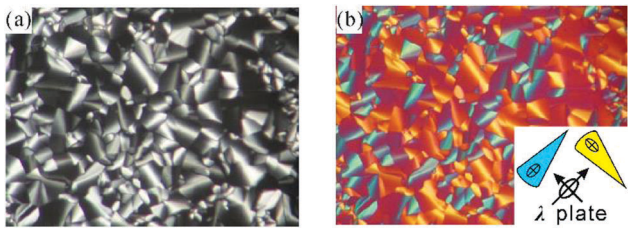

Fig. 1 Polarized optical microscopy textures of **IC^3/14** at 70 °C. (b) is recorded with a full-wave (λ) plate. For explanation of colours see ESI.†

Table 1 The phase transition temperatures of compounds **IC^3/*n***[a]

Compd	*n*	*T*/°C [Δ*H*/kJ mol^{-1}]
IC^3/10	10	↑Cr_1 69.6 [17.3] Cr_2 107.0 [33.3] Iso ↓ 87.4 [1.2] *p*31*m* 52.8 [12.0] M ↑ 56.5 [12.3] *p*3 + Cr_1 65.4 [2.4] *p*31*m* 90.3 [1.2] Iso + Cr_2 108.6 [3.3] Iso
IC^3/12	12	↑ Cr_1 86 [21.1] Cr_2 110.2 [41.5] Iso ↓ 88.6 [0.7] *p*31*m* 58.3 [11.5] M ↑62.1 [11.6] *p*31*m* 89 Cr_2 110.3 [35.7] Iso
IC^3/14	14	↑Cr_1 38.7 [30.5] Cr_2 73 [23.1] *p*31*m* 82.7 [0.8] Iso ↓76.2 [0.3] *p*31*m* 58.5 [14.6] M ↑ 62.5 [14.7] *p*31*m* + Cr_2 68.2 [1.0] *p*31*m* 83.9 [0.6] Iso

[a] Peak DSC transition temperatures [and enthalpies] on 1st heating (↑), followed by cooling (↓), followed by 2nd heating (↑), all at 5 K min^{-1}. Cr_1, Cr_2 = crystal, *p*31*m* = hexagonal columnar phase with three-fold symmetry, Iso = isotropic melt, and M is a complex metastable unidentified LC phase.

studies, are listed in Table 1. The DSC traces are shown in Fig. S1 and S2 of ESI.†

All of the target compounds **IC^3/*n*** were synthesized by click reaction between the bisacetylene 8 and the appropriate substituted aromatic azides **5^3/*n*** (Scheme 1). Reduction of commercially available 4,4′-dihydroxybenzophenone **6** with $LiAlH_4/AlCl_3$[19] yielded 4,4′-dihydroxydiphenylmethane **7**, which was etherified with propargylbromide to yield bisacetylene **8.** 4-Azidophenol **4** was synthesized from commercially available 4-aminophenol **3** by formation of the diazonium salt and subsequent substitution with sodium azide.

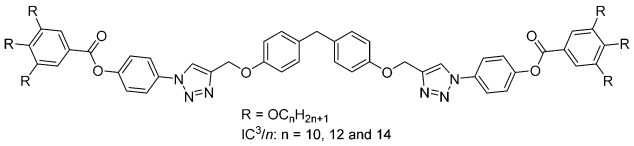

4 was esterified with the appropriate 3,4,5-trialkoxybenzoic acids **2^3/*n*** to 4-azidophenyl-3,4,5-trialkoxybenzoates **5^3/*n***.[20] Finally click reaction between bisacetylene 8 and aromatic azides **5^3/*n*** produced the target compounds **IC^3/*n*.** All of the target compounds were purified by column chromatography. For more details, see ESI.†

X-ray scattering at small and wide angles (SAXS and WAXS) experiments were performed to characterize the LC phases. Grazing incidence SAXS (GISAXS) on well oriented thin films on silicon facilitated indexing of X-ray reflections.

Furthermore, for any potential future application of such materials in electronic or optical devices, orientation in thin film needs to be understood. Fig. 2 shows a transmission powder SAXS and a GISAXS pattern of the main liquid crystal phase, on the example of **IC^3/12.** Equivalent patterns for compounds **IC^3/10** and **IC^3/14** are shown in ESI,† Fig. S4–S6. The measured and calculated *d*-spacings for all three compounds are listed in Tables S1–S3 in ESI.† The d^{-2} values of the three peaks in the SAXS pattern are in the ratio 1 : 3 : 4, which is typical of a two-dimensional hexagonal lattice, with the respective Miller indices (10), (11) and (20). The GISAXS patterns confirm this indexing, as seen in Fig. 2b and Fig. S4a, S5a (ESI†). The fact that the reflections are not confined to the equatorial plane means that the columns are oriented parallel to the substrate surface (planar anchoring), rather than perpendicular to it. This is consistent with the appearance of the optical micrographs in Fig. 1 and Fig. S3 (ESI†). As the real space unit cell is related to the reciprocal cell by 90° rotation, the fact that reflections (10) and (20) are on the meridian means that the real hexagonal cell lies on one of its sides on the substrate. That implies that the (10) plane is parallel to the substrate, suggesting in turn that it is the most densely packed plane (see Fig. S9, ESI†).[21] In compounds **IC^3/12** and **IC^3/14** another metastable mesophase (M-phase) has been observed in rapidly cooled samples. The GISAXS pattern is presented in Fig. S7 (ESI†). The structure of this complex phase is not clear at present, and is the subject of further investigations.

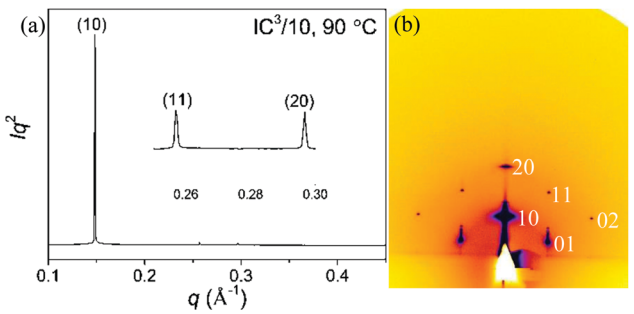

Fig. 2 (a) Powder SAXS curve of **IC^3/12** recorded at 80 °C at station I22 at Diamond. (b) GISAXS diffraction pattern of **IC^3/12** recorded at 80 °C on beamline B28 at ESRF.

Table 2 Comparison of the values of lattice parameter (in nm) of the hexagonal columnar phase in the three compounds at different temperatures

Compound	60 °C	70 °C	80 °C	90 °C
IC^3/10	5.03	4.98	4.94	4.89
IC^3/12	5.23	5.18	5.13	
IC^3/14	5.41	5.35	5.28	

The lattice parameters of **IC^3/10**, **IC^3/12** and **IC^3/14** at different temperatures are listed in Table 2. As expected, the value of lattice parameter a is seen to increase with increasing end-chain length. The continuous trend suggests that the basic phase structure is the same in all three compounds. It is also seen in Table 2 that a decreases with increasing temperature, a common trend observed in columnar phases, particularly those containing a large aliphatic fraction.[12]

In order to determine the molecular arrangement in the columnar phase, we first need to establish the orientation of the molecular cores relative to the column axis and then determine the number of molecules in the unit cell. Using the λ retardation plate (Fig. 1b and Fig. S3b, d, f, ESI†) we confirm that the slow axis, hence the long axis of the aromatic core, is perpendicular to the column axis (see ESI†). For the calculation of the number of molecules refer to Table S4 in ESI.† To estimate molecular volume in the LC phase the molecule is split in two parts. The volume of the rigid aromatic part is estimated using the methods of crystalline volume increments.[22] For the aliphatic part the density of 0.8 g cm^{-3} is assumed, being in between the values for liquid *n*-alkanes and amorphous polyethylene. From the measured area of the unit cell and an assumed intermolecular spacing along the column axis c in the usual range between 0.4 and 0.45 nm, we obtain close to 3 as the number of molecules per unit cell. As we don't know the actual value of c (no sharp feature is observed in the 0.3–0.5 nm WAXS range), in Table S4 (ESI†) we give the calculated value of c assuming that the number of molecules, which must be an integer, is exactly 3. As can be seen, the value of c is in the range between 0.407 and 0.433, increasing slightly with the length of the terminal chains.

With the above in mind, we consider two alternative models of molecular packing. In both models three molecules cluster together in one stratum, with their aromatic cores back-to-back, forming a three-arm star. The models differ in the arrangement of the star-profiled columns. In model A the centres of the stars are situated at apices of hexagons, producing a hexagonal honeycomb with aromatic walls where the central methylene groups occupy alternative corners of the hexagon. This packing model resembles that found in anchor-shaped mesogens consisting of a bent-rod aromatic core with a flexible chain attached to the inside of the bend point.[15] However, while in the case of anchor mesogens the ends of the aromatic arms were linked *via* hydrogen-bonding terminal groups, the present compounds do not. In fact the bulky end-chains on adjacent molecules would face each other and clash, having to bend sharply in order to fill the interior of the hexagonal channel. Even rotating the star-like columns by 60° about their axis does not solve the packing problem as tested by molecular simulation.

In the alternative model (B) the self-assembled stars are located on a triangular lattice all with the same orientation – see the models

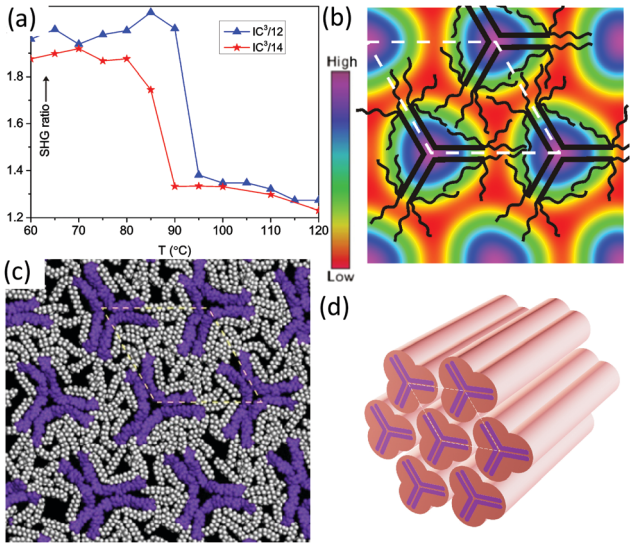

Fig. 3 The Col/$p31m$ phase: (a) temperature dependent intensity of the second harmonic (400 nm) *vs.* background for 800 nm excitation, generated 20 μm above the substrate surface in **IC^3/12** and **IC^3/14**; (b) electron density map, with schematic molecules overlaid; (c) snapshot of molecular dynamic simulation: purple = aromatic, grey and white = aliphatic chains (see Video in ESI†); (d) schematic of the Col/$p31m$ phase. In (b and c) the view is down the columns. Note that according to the GISAXS pattern in Fig. 2b and Fig. S4a, S5a (ESI†) the column orientation in this figure is as in a film on a horizontal substrate viewed along the substrate surface (see Fig. S9 in ESI†).

in Fig. 3b–d. This arrangement is favoured for steric reasons, as the bunch of six alkyls emanating from the end of a star arm faces the empty concave "armpit" of the adjacent column. To test the viability of the two arrangements and their variants, molecular models of crystals were built with the experimental unit cell parameter a and with c from Table S4 (ESI†). These were then subjected to molecular dynamics annealing. Space could not be filled uniformly with model A, while a very satisfactory density distribution was achieved with model B – see snapshot in Fig. 3c. A short video of the dynamics of model B is available from the ESI.†

The columnar structure in Fig. 3 has 3-fold rather than 6-fold symmetry, and the plane group is $p31m$ rather than the usual $p6mm$ symmetry of the Col$_{hex}$ phase. While the $p6mm$ plane group has a centre of inversion, $p31m$ has not. To distinguish between them, we performed second harmonic generation (SHG) experiments. Fig. 3a shows a large increase in SHG signal above the background level on cooling from Iso to Col$_{hex}$ phase, showing clearly that the latter phase lacks centre of symmetry and is thus a trigonal phase (see also ESI†).

The lack of centre of symmetry causes a problem when reconstructing the electron density (ED) map from X-ray diffraction intensities. That is, the phase ϕ of the structure factor of one of the three reflections, the (11), is not limited to 0° or 180°, a condition that applies to all reflections in centrosymmetric space groups. A value of ϕ different from 0° or 180° breaks the hexagonal symmetry. Choosing an arbitrary angle ϕ = 120° we obtain the ED map in Fig. 3b, onto which the schematic molecules of an **IC^3/*n*** compound are superimposed. The high density regions (purple) represent the aromatic moieties, and the blur comes from the time

and space averaging in the liquid crystal. We note that choosing a different value of ϕ merely changes the extent of deviation from circularity of the high-density maxima – see Fig. S8 (ESI†).

We consider that the efficient back-to-back packing of the three bent cores in this structure is facilitated by a degree of flexibility in the core, particularly around the oxymethylene linkage. The long-range polarity, on the other hand, is believed to be secured by the high barrier for uncorrelated rotation around the column axis.

It is interesting to compare the present structure with that of a bent-core phasmid compound also having six terminal $C_{14}H_{29}$ chains but with longer arms and a pyridine ring as the bend point.[23] The model proposed for the hexagonal phase had four rather than three molecules in a stratum resulting in a 4-arm star. *p*6*mm* symmetry was assumed. Interestingly, at lower temperatures a phase transition to a polar columnar phases took place but unlike in the current case, the poling was parallel rather than perpendicular to the column axis. Longitudinal poling was explained by an out-of-plane distortion of the stars.

It is also appropriate to compare the present structure with those of a number of mesogens with 3-fold (C_3) symmetry in their chemical structure. In the columnar phase of the 3-arm star molecules by Lehmann *et al.*[24] the molecules are actually thought to be distorted into an E-shaped conformation, making them effectively fan-shaped and thus assembling as other fan-shaped mesogens such as dendrons. In other cases the fact that the non-centrosymmetric 3-arm star molecules of C_3 symmetry formed the Col_{hex} phases was thought to be the result of rotational averaging.[25] However, even though the diffraction pattern has hexagonal symmetry, this does not preclude the real-space structure having only trigonal symmetry. One has to remember that the Laue symmetry (*i.e.* the symmetry of the diffraction pattern) is hexagonal even if the crystal symmetry is trigonal. Indeed the columnar phase of compounds described in ref. 26 showed strong second harmonic generation (SHG), characteristic of non-centrosymmetric structures. In other reported cases of C_3 star-like mesogens only 6-fold symmetry was claimed for the columnar LC phase.[26–28]

As hinted in the introduction, beside the already mentioned trigonal columnar phase in anchor-shaped compounds,[15] there has been another case of triangular honeycomb LC of straight rod amphiphiles, where two incompatible side-chains were attached at each side of the aromatic rod.[16] While at higher temperatures the two chain types were mixed in the triangular channels, a second-order Curie-type transition on cooling brought about a trigonal *p*31*m* phase in which the two side-chain types were separated in triangles on two separate sublattices. A recent Monte Carlo simulation helps understand such *p*6*mm*–*p*31*m* transitions.[29]

In summary, we have synthesised a series of bent-core phasmid compounds and found that they form a trigonal columnar phase, where the aromatic columns adopt a 3-armed star-shaped cross-section. This finding indicates a potential new path to creating non-centrosymmetric self-assemblies that could, with suitable substituents, be used in ferroelectric, pyroelectric or frequency-doubling optical devices.

The authors acknowledge funding for this work from EPSRC (EP-K034308, EP-P002250), NSFC (No. 21664015, 21364017, 21602195) and YEDF (ZD2015001). YL thanks CSC for stipend and UoS for waiving tuition fee. For help with synchrotron experiments we thank Prof. N. Terrill and Dr O. Shebanova, beamline I22, Diamond Light Source, and Drs O. Bikondoa, S. Brown and P. Thompson of beamline BM28 at ESRF.

Conflicts of interest

There are no conflicts to declare.

References

1 H. T. Nguyen, C. Destrade and J. Malthête in *Handbook of Liquid Crystals*, ed. D. Demus, J. Goodby, G. W. Gray, H. W. Spiess, V. Vill, *Wiley-VCH Verlag GmbH*, 1998, p. 865.
2 D. Fazio, C. Mongin, B. Donnio, Y. Galerne, D. Guillon and D. W. Bruce, *J. Mater. Chem.*, 2001, **11**, 2852.
3 T. Woehrle, I. Wurzbach, J. Kirres, A. Kostidou, N. Kapernaum, J. Litterscheidt, J. C. Haenle, P. Staffeld, A. Baro, F. Giesselmann and S. Laschat, *Chem. Rev.*, 2016, **116**, 1139.
4 W. Pisula, M. Zorn, J. Y. Chang, K. Müllen and R. Zentel, *Macromol. Rapid Commun.*, 2009, **30**, 1179.
5 M. O'Neill and S. M. Kelly, *Adv. Mater.*, 2011, **23**, 566.
6 M. Funahashi, *J. Mater. Chem. C*, 2014, **2**, 7451.
7 T. Kato, M. Yoshio, T. Ichikawa, B. Soberats, H. Ohno and M. Funahashi, *Nat. Rev. Mater.*, 2017, **2**, DOI: 10.1038/natrevmats.2017.1.
8 C. Tschierske, *Angew. Chem., Int. Ed.*, 2013, **52**, 1.
9 G. Ungar, C. Tschierske, V. Abetz, R. Holyst, M. A. Bates, F. Liu, M. Prehm, R. Kieffer, X. B. Zeng, M. Walker, B. Glettner and A. Zywocinski, *Adv. Funct. Mater.*, 2011, **21**, 1296.
10 C. Dressel, F. Liu, M. Prehm, X. B. Zeng, G. Ungar and C. Tschierske, *Angew. Chem., Int. Ed.*, 2014, **53**, 13115.
11 E. Fontes, P. A. Heiney and W. H. Jeu, *Phys. Rev. Lett.*, 1988, **61**, 1202.
12 J. K. Kwon, S. N. Chvalun, J. Blackwell, V. Percec and J. A. Heck, *Macromolecules*, 1995, **28**, 1552.
13 M. A. Shcherbina, X. B. Zeng, T. Tadjiev, G. Ungar, S. H. Eichhorn, K. E. S. Phillips and T. J. Katz, *Angew. Chem., Int. Ed.*, 2009, **48**, 7837.
14 V. Percec, *et al.*, *J. Am. Chem. Soc.*, 2011, **133**, 12197.
15 B. Glettner, F. Liu, X. B. Zeng, M. Prehm, U. Baumeister, G. Ungar and C. Tschierske, *Angew. Chem., Int. Ed.*, 2008, **47**, 6080.
16 X. B. Zeng, *et al.*, *Science*, 2011, **331**, 1302.
17 H. C. Kolb, M. G. Finn and K. B. Sharpless, *Angew. Chem., Int. Ed.*, 2001, **40**, 2004; C. W. Tornøe, C. Christensen and M. Meldal, *J. Org. Chem.*, 2002, **67**, 3057.
18 Y. Bouligand, *J. Phys.*, 1980, **41**, 1297.
19 A. K. Boal and V. M. Rotello, *J. Am. Chem. Soc.*, 2002, **124**, 5019.
20 X. Tan, L. Kong, H. Dai, X. Cheng, F. Liu and C. Tschierske, *Chem. – Eur. J.*, 2013, **19**, 16303.
21 G. Ungar, F. Liu, X. B. Zeng, B. Glettner, M. Prehm, R. Kieffer and C. Tschierske, *J. Phys.: Conf. Ser.*, 2010, **247**, 012032.
22 A. Immirzi and B. Perini, *Acta Crystallogr., Sect. A: Cryst. Phys., Diffr., Theor. Gen. Crystallogr.*, 1977, **33**, 216.
23 J. Matraszek, J. Mieczkowski, D. Pociecha, E. Gorecka, B. Donnio and D. Guillon, *Chem. – Eur. J.*, 2007, **13**, 3377.
24 M. Lehmann and M. Jahr, *Chem. Mater.*, 2008, **20**, 5453.
25 G. Hennrich, A. Omenat, I. Asselberghs, S. Foerier, K. Clays, T. Verbiest and J. L. Serrano, *Angew. Chem., Int. Ed.*, 2006, **45**, 4203.
26 E. Beltran, J. L. Serrano, T. Sierra and R. Gimenez, *J. Mater. Chem.*, 2012, **22**, 7797.
27 S. K. Pathak, R. K. Gupta, S. Nath, D. S. S. Rao, S. K. Prasad and A. S. Achalkumar, *J. Mater. Chem. C*, 2015, **3**, 2940.
28 E. Westphal, M. Prehm, I. H. Bechtold, C. Tschierske and H. Gallardo, *J. Mater. Chem. C*, 2013, **1**, 8011.
29 S. George, C. Bentham, X. B. Zeng, G. Ungar and G. A. Gehring, *Phys. Rev. E*, 2017, **95**, 062126.